HHS Public Access

Author manuscript

Am J Transplant. Author manuscript; available in PMC 2021 January 01.

Published in final edited form as:

Am J Transplant. 2020 January ; 20(1): 75–87. doi:10.1111/ajt.15517.

Circulating T Follicular Helper Cells Are a Biomarker of Humoral Alloreactivity and Predict Donor-Specific Antibody Formation After Transplantation

G. Michael La Muraglia II[1], **Maylene E. Wagener**[1], **Mandy L. Ford**[1], **I. Raul Badell**[1,*]

[1]Emory Transplant Center, Atlanta, GA, USA

Abstract

Donor-specific antibodies (DSA) contribute to renal allograft loss. However, biomarkers to guide clinical management of DSA post-transplant or detect humoral alloimmune responses before alloantibodies develop are not available. Circulating T follicular helper (Tfh) cells are $CD4^+CXCR5^+$ Tfh-like cells in the blood that have been associated with alloantibodies in transplant recipients, but whether they precede antibody formation for their evaluation as a predictive biomarker in transplantation is unknown. To evaluate the ability of circulating Tfh (cTfh) cells to predict DSA, we utilized murine transplant models to determine the temporal relationship between cTfh cells, germinal center (GC) formation, and DSA development. We observed that donor-reactive $CD4^+CXCR5^+$ cTfh cells expand following allotransplantation. These cTfh cells were equivalent to graft-draining lymph node-derived Tfh cells in their ability to provide B cell help for antibody production. Circulating Tfh cell expansion and differentiation into $ICOS^+PD\text{-}1^+$ cells temporally correlated with GC alloreactivity and preceded the generation of DSA in instances of modified and unmodified alloantibody formation. Importantly, delayed costimulation blockade initiated after the detection of $ICOS^+PD\text{-}1^+$ cTfh cells prevented DSA. These findings suggest that cTfh cells could serve as a biomarker for humoral alloreactivity prior to the detection of alloantibodies and inform therapeutic approaches to prevent DSA.

1. Introduction

Over the last several decades, advances in solid organ transplantation have significantly reduced acute rejection rates leading to great improvements in short-term kidney allograft survival (1). However, long-term outcomes following kidney transplantation remain suboptimal. Historically, late kidney allograft failure was chiefly attributed to calcineurin inhibitor toxicity and chronic allograft nephropathy (2), but it is now well recognized that donor-specific HLA antibodies are an important immunologic cause of acute and chronic allograft injury that shorten renal allograft survival (3). These anti-HLA donor-specific antibodies (DSA) exist either pre-transplant or arise *de novo* after transplant and are

*Corresponding Author: I. Raul Badell, ibadell@emory.edu.

Disclosures

The authors of this manuscript have no conflicts of interest to disclose as described by the *American Journal of Transplantation*.

Data Availability Statement

The data that support the findings of this study are available from the corresponding author upon reasonable request.

associated with inferior transplant outcomes (4, 5). Despite the prevalence and deleterious impact of HLA antibodies in kidney transplantation, diagnostic biomarkers to reliably guide clinical management of pathologic DSA have not been developed (6).

While the availability of sensitive assays for the identification of HLA antibodies has greatly enhanced pre-transplant donor-recipient matching to reduce the incidence of early antibody-mediated rejection (7), their utility in the post-transplant setting has been limited (8, 9). Once anti-donor antibodies are detected, reproducible therapeutic options to curtail the natural history of antibody-mediated kidney allograft injury are not clinically available (3, 6). Therefore, the value of detecting DSA to either direct the initiation of treatment strategies aimed at inhibiting alloantibody-mediated injury or measure the effectiveness of such strategies is lacking. As such, there is great need for the development of alternative biomarkers that can diagnose the presence of humoral alloimmunity in kidney transplant recipients and facilitate the initiation of therapeutic interventions to prevent premature allograft loss.

T follicular helper (Tfh) cells are a lineage of $CD4^+$ T cells distinguishable by their unique expression of the chemokine receptor CXCR5 and are required for the provision of B cell help to generate class-switched, high affinity antibody responses for an effective humoral immune response (10). Tfh cells have now been implicated in many immune processes during health and disease (11), and inhibition of their differentiation and function prevents the development of anti-donor antibody responses in transplantation (12–14). Hence the detection of Tfh cells as a new biomarker for alloantibodies in transplantation is theoretically appealing, but access to Tfh cells is limited in humans because they are primarily present in secondary lymphoid organs (SLO) and are therefore not accessible via non-invasive methods for diagnostic purposes. However, newly identified $CD4^+CXCR5^+$ circulating Tfh (cTfh) cells in peripheral blood have been recently shown to correlate with vaccine responses and autoimmune disease activity in experimental animal models and humans (15, 16), and thus may overcome this barrier to accessibility. Although there have been a few observational reports associating cTfh cells with alloantibodies in transplant recipients (17–19), the temporal relationship of cTfh cells to DSA and their ability to function as a predictive biomarker in transplantation is unknown.

In this study, we used murine transplant models to test the ability of cTfh cells to predict the development of alloantibodies by determining the temporal relationship between both polyclonal endogenous and antigen-specific cTfh cells, germinal center (GC) reactivity and DSA formation. We demonstrate that alloreactive $CXCR5^+$ $CD4^+$ T cells detected in the blood after transplant are phenotypically and functionally cTfh cells. The expansion kinetics of donor-reactive cTfh cells and their phenotypic differentiation into $ICOS^+PD\text{-}1^+$ cells temporally correlated with GC alloreactivity and predicted the generation of DSA. Delayed treatment with costimulation blockade initiated after transplant upon the detection of $ICOS^+PD\text{-}1^+$ cTfh cells successfully inhibited alloantibody formation. Thus alloreactive cTfh cells could potentially serve as a clinical biomarker for nascent or ongoing humoral alloimmune responses before the detection of anti-donor antibodies and inform therapeutic approaches to prevent DSA.

2. Materials and Methods

2.1 Mice

B6-Ly5.1/Cr (H2-K^b) and BALB/c (H-2K^d) mice were obtained from the National Cancer Institute. Ovalbumin (OVA)-specific TCR transgenic OT-I (20) and OT-II (21) mice purchased from Taconic Farms were bred to Thy1.1$^+$ background from The Jackson Laboratory at Emory University. C57BL/6 mice that constitutively express membrane-bound OVA (mOVA) under the β-actin promoter (22) were a gift from M. Jenkins (University of Minnesota). All animals were housed in pathogen-free facilities and maintained in accordance with Emory University Institutional Animal Care and Use Committee guidelines.

2.2 T cell adoptive transfers, skin transplantation, and immunosuppression

For adoptive transfers of OVA-specific T cells, splenocytes isolated from Thy1.1$^+$ OT-I and Thy1.1$^+$ OT-II mice were quantified via TruCount bead analysis (BD Biosciences) and 1.0×10^6 of each Thy1.1$^+$ OT-I and Thy1.1$^+$ OT-II T cells was injected intravenously into naïve B6-Ly5.1/Cr mice 24–48 hours prior to skin transplantation. Bilateral dorsal full-thickness tail and ear skin were transplanted onto recipient mice (23). Skin graft recipients received no treatment, anti-CD28 domain antibody (dAb) (100 μg, Bristol-Myers Squibb), CTLA-4-Ig (200 μg, Bristol-Myers Squibb), or tacrolimus (5 mg/kg, Astellas). Anti-CD28 dAb and CTLA-4-Ig were administered intraperitoneally on post-transplant days 0, 2, 4, 6 and 8 and then weekly. Delayed anti-CD28 dAb was administered on days 7, 9, 11, 13 and 15 and then weekly. Tacrolimus was administered s.c. daily with mean trough levels of 7.1 ± 3.2 ng/mL.

2.3 Flow cytometry

Graft-draining axillary and brachial lymph nodes were processed into single-cell suspensions. Peripheral blood mononuclear cells (PBMC) were isolated by Ficoll-Paque (GE Healthcare) density gradient centrifugation of whole blood preparations. Cells were surface stained for indicated markers and pulsed with LIVE/DEAD viability dye (Molecular Probes) before fixation. Intracellular staining was performed with Foxp3 Fixation/Permeabilization Buffer Kit (eBioscience). All antibodies were from BioLegend and BD Biosciences. All samples were run on an LSR Fortessa flow cytometer (BD Biosciences) and analyzed by using FlowJo Software (Flowjo, LLC). CountBright Beads (Invitrogen) were used to determine absolute cell counts.

2.4 T:B cell co-culture

T and B cells from blood and graft-dLNs were enriched, flow sorted and co-cultured as previously described (24). Briefly, magnetic bead negative selection (Miltenyi Biotec) was used to enrich CD4$^+$ T and CD19$^+$ B cells. T cells from dLNs were flow sorted into CXCR5$^-$(CD19$^-$CD4$^+$PD-1^{int}CXCR5$^-$GITR$^-$) and Tfh (CD19$^-$CD4$^+$PD-1^{hi}CXCR5$^+$GITR$^-$) cells, and from blood into CXCR5$^-$(CD19$^-$CD4$^+$CXCR5$^-$GITR$^-$) and cTfh (CD19$^-$CD4$^+$CXCR5$^+$GITR$^-$) cells on a FACSAria II (BD Biosciences). 3×10^4 T cells were cultured with 5×10^4 B cells in 96-well plates in anti-CD3e (2C11, 2 μg/mL, BioXcell) and

anti-IgM (5 μg/mL, Jackson Immunoresearch) containing media for 6 days. Cultured cells were analyzed by flow cytometry and supernatants for total IgG levels by ELISA.

2.5 Anti-donor antibody assessment

For flow cytometric crossmatch, BALB/c splenocytes were processed into single-cell suspensions and pre-treated with Fc Block (BioLegend), followed by incubation with recipient serum at 4°C. Splenocytes were then washed and labeled with surface markers and anti-mouse IgG (BioLegend) for quantification of anti-BALB/c IgG by flow cytometry. For ELISA anti-OVA antibody measurements, flat-bottom 96-well Immulon 4HBX microtiter plates (VWR) were coated with OVA protein (100 μg/well; Sigma-Aldrich) overnight at 4°C, blocked with 10% FBS in PBS-T for 1 hour at 37°C, and then incubated with serum samples for 1.5 hours at 37°C. OVA-specific immunoglobulins were detected with HRP goat anti-mouse IgG (Poly4053, BioLegend), developed by using the TMB substrate system (Thermo Scientific), and read at 450 nm on a Spectra MAX 340PC Microplate reader (Molecular Devices).

2.6 Statistical analysis

The Mann–Whitney U nonparametric t test was performed for analysis of unpaired groups, and the Holms–Sidak method was used for grouped, multiple t test analyses. All analyses were performed by using GraphPad Prism (GraphPad Software, Inc.). Statistical significance was attributed to p values <0.05 (*<0.05, **<0.01, ***<0.001).

3. Results

3.1 CXCR5$^+$ CD4$^+$ T cells are detectable in the blood, expand after transplant, and exhibit phenotypic and functional characteristics of cTfh cells

To interrogate the CXCR5$^+$ CD4$^+$ T cell response in the blood following transplantation we utilized a full MHC mismatch BALB/c to B6 murine skin transplant model (Figure 1A). Naïve B6 recipients were transplanted bilateral full thickness skin grafts from either syngeneic (B6) or allogeneic (BALB/c) donor mice and sacrificed 10 days post-transplant for PBMC and graft-draining lymph node (dLN) analysis. CXCR5$^+$ CD4$^+$ T cells were identified in the blood posttransplant (Figure 1B) and exhibited robust expansion in response to the BALB/c allograft as compared to the syngeneic B6 graft (Figure 1C). Analysis of these CXCR5$^+$ CD4$^+$Foxp3$^-$ T cells revealed a less polarized but similar phenotype to graft-dLN CXCR5$^+$PD-1^{hi} Tfh cells (Figures 1D, E), and a distinct phenotype from other circulating naïve and antigen-experienced CD4$^+$ T cells (Figure 1F). They exhibited greater expression of the Tfh markers CXCR5, PD-1, TCF-1, TIGIT and GL-7 relative to antigen-experienced (CD44^{hi}CXCR5$^-$) CD4$^+$ T cells (10, 25), as well as increased expression of the costimulatory molecules CD28 and ICOS, and the proliferation marker Ki–67.

To test the ability of these circulating CXCR5$^+$ T cells to provide B cell help, we performed in vitro T:B cell co-cultures of donor-reactive CXCR5$^-$ and CXCR5$^+$ CD4$^+$CD44$^+$ T cells from the blood and dLNs of transplanted mice. In contrast to CXCR5$^-$ cells, circulating CXCR5$^+$ cells induced GC-like B cell differentiation, class switching and IgG antibody production equivalent to their CXCR5$^+$ Tfh cell DLN counterparts (Figures 1G, H). Taken

together, these data indicate that alloreactive CXCR5$^+$ CD4$^+$ T cells in the peripheral blood are indeed cTfh cells that expand in response to an allograft and display the unique phenotypic and functional characteristics of Tfh cells (16, 26–28).

3.2 Circulating Tfh cell kinetics parallel graft-dLN GC reactivity after transplantation

The idea of utilizing cTfh cells as a surrogate marker for GC activity and protective antibody formation in SLOs has been introduced in HIV and influenza vaccination (28, 29). To begin to investigate whether cTfh cells could serve as a potential indicator of GC activity in transplantation, we transplanted B6 recipient mice with syngeneic (B6) or allogeneic (BALB/c) skin grafts and measured cTfh cell kinetics in relation to GC Tfh and B cell reactivity in graft-DLNs. We detected a rise in the frequency and number of cTfh cells that peaked on day 10 and contracted by day 21 (Figures 2A, B). Similarly, GC alloreactivity as measured by Tfh cell differentiation and GC B cell expansion in the DLNs also peaked 10 days after transplant with contraction beginning by day 14 (Figures 2A, C, D). Graft-elicited antibody secreting plasmablasts and plasma cells peaked 10 days post-transplant (Figures 2A, E, F), while memory B cells (IgG$^-$ and IgG$^+$ CD19$^+$IgD$^-$B220$^+$CD38$^+$CD80$^+$ cells) did not exhibit any significant changes over time (data not shown). Collectively, these data show that cTfh cell kinetics reliably reflect GC kinetics in SLOs (Figure 2G) and therefore could potentially be used as a biomarker for GC reactivity in the peripheral blood.

3.3 Donor-reactive cTfh cells exhibit an activated ICOS$^+$PD-1$^+$ phenotype after transplantation

Due to previously described heterogeneity of CXCR5$^+$ cTfh cells in relation to antigen exposure or disease activity (11, 30), we sought to determine whether phenotypic differences developed within the cTfh cell subset after transplantation. Thus, we examined the cTfh cell phenotype in naïve and syngeneic or allogeneic skin-grafted mice 10 days post-transplantation. Phenotypic analysis revealed significant differences in the expression of the Tfh activation markers PD-1 and ICOS on cTfh cells in response to an allograft as compared to an isograft or in naïve mice (Figure 3A). This observation prompted the assessment of PD-1 and ICOS co-expression on these cTfh cells (Figure 3B). Interestingly, we observed that the alloreactive cTfh cells were composed of a significantly greater fraction of ICOS $^+$PD-1$^+$ cells (Figures 3C, D), and that the increase in frequency and number of cTfh cells with this polarized phenotype resulted from alloantigen exposure, as the phenotype did not manifest in syngeneic-grafted or naïve mice. This ICOS$^+$PD-1$^+$ cTfh cell population showed greater expression of CXCR5, TCF-1, CD154, Ki-67, GL-7 and other markers of Tfh cell activation as compared to less polarized ICOS$^-$PD-1$^-$c Tfh cells (Figure 3E). Intriguingly, this ICOS$^+$PD-1$^+$ cTfh cell subset began to manifest as early as 7 days after transplant, with a 3-fold increase over baseline (day 0) by day 7 and 4-fold increase at the peak of the GC response on day 10 (Figures 3F–H). These findings indicate that cTfh cells develop a distinguishable activated phenotype after allotransplantation that emerges earlier (day 7) than the discernible rise in the quantity of cTfh cells (day 10, Figure 2) and could predict alloantibody formation.

3.4 Circulating Tfh cells precede DSA formation after transplantation

Based on the observation that detectable changes in the quantity and quality of cTfh cells correspond with GC alloreactivity (Figures 2, 3), we next sought to determine the kinetics of DSA formation in our model. Naïve B6 recipients received either B6 or BALB/c skin grafts and were serially bled for serum collection and flow crossmatch analysis to test for the development of anti-donor antibodies. As expected, the syngeneic graft recipients did not develop DSA, while the allogeneic graft recipients formed anti-BALB/c alloantibodies by posttransplant day 14 with peak titers by day 28 (Figures 4A, B). Comparison of our observed cTfh cell kinetics to the onset of DSA formation demonstrates that the rise in frequency and number of cTfh cells in the blood begins and peaks before DSAs are first detectable in the serum 14 days after transplant (Figure 4C). Interestingly, manifestation of the activated $ICOS^+PD\text{-}1^+$ phenotype within the cTfh cell population occurs even earlier (day 7, Figure 3) than the increase in total alloreactive cTfh cells (day 10, Figure 2) and precedes the generation of DSA by 7 days (Figure 4D). Thus, changes in the quantity of cTfh cells and their phenotype could provide a non-invasive means of predicting *de novo* DSA formation following transplantation.

3.5 Antigen-specific TCR transgenic cTfh cells display similar phenotypic characteristics and kinetics to endogenous alloreactive cTfh cells following transplantation

We previously reported that donor-reactive endogenous Tfh cells in graft-dLNs exhibited the same phenotypic and differentiation characteristics as transgenic antigen-specific Tfh cells in response to a donor skin graft (14). To characterize the antigen-specific cTfh cell response, we utilized our established TCR transgenic mOVA murine skin transplant model (31) to track donor-specific TCR transgenic cTfh cells. $Thy1.1^+$ $CD4^+$ OT-II and $CD8^+$ OT-I T cells were adoptively transferred into naive B6 mice, which were then transplanted with skin from either syngeneic (B6) or minor antigen-mismatched (mOVA) donors (Figure 5A). Mice were then serially sacrificed for PBMC, dLN and serum analyses. OVA-specific $Thy1.1^+CXCR5^+$ cTfh cells were detected in the peripheral blood in response to the mOVA grafts but not the B6 isografts (Figures 5B, C), peaking in frequency and number 10 days after transplant. They exhibited a Tfh-like phenotype with increased expression of CXCR5, PD-1, and ICOS relative to $Thy1.1^+CXCR5^-$ and naïve $CD4^+$ OT-II T cells (Figure 5D). Notably, these antigen-specific OT-II cTfh cells were composed of a substantial proportion of $ICOS^+PD\text{-}1^+$ cells (Figures 5E, F) that were detectable 7 days after transplant (Figure 5G). Examination of the OT-II Tfh cell response in the graft-dLNs correlated with $Thy1.1^+$ cTfh cell kinetics (data not shown), and most importantly, the rise in antigen-specific cTfh cells in the blood preceded the development of anti-OVA DSA in mOVA graft recipients (Figures 5H, I). As such, TCR transgenic donor-specific cTfh cells manifest similar phenotypic features and expansion kinetics to endogenous, alloreactive cTfh cells in relation to the generation of DSA.

3.6 Circulating Tfh cells predict breakthrough alloantibodies despite immunosuppression

Preventing *de novo* DSA in our mouse skin graft models with immunomodulatory therapy correlates with GC inhibition in the dLNs (14), but the impact of immunosuppression on alloreactive cTfh cells and their ability to predict DSA is not known. Hence, we sought to

determine the relationship between cTfh cells, immunosuppression, and DSA inhibition. Naïve skin-grafted mice were treated with CD28 costimulation blockade (CoB, CTLA-4-Ig or anti-CD28 dAb), tacrolimus, or left untreated. Peripheral blood analysis on post-transplant day 10 showed that immunosuppression resulted in significant reductions in the frequency and number of total cTfh cells and the $ICOS^+PD\text{-}1^+$ cTfh cell subset observed in response to an allogeneic graft as compared to untreated controls (Figures 6A–D). Tfh and GC B cells in the graft-dLNs were also reduced (Figures 6E, F), along with complete inhibition of DSA formation with the more potent anti-CD28 dAb (Figure 6G). Importantly, cTfh cell quantity and phenotype positively correlated with breakthrough GC reactivity and preceded DSA under less potent CNI- and CoB-based immunosuppression with tacrolimus and CTLA-4-Ig (Figures 6A–G). Therefore, alloreactive cTfh cell expansion and phenotypic differentiation predicted DSA in instances of both modified (CNI and CoB) and unmodified alloantibody formation.

3.7 Delayed anti-CD28 CoB initiated after detection of $ICOS^+PD\text{-}1^+$ cTfh cells prevents DSA formation

Having determined that cTfh cells predict DSA in our model, we next tested whether initiating immunosuppression after transplant upon the detection of alloreactive cTfh cells could prevent the generation of alloantibodies. Naïve B6 mice were transplanted BALB/c skin and their blood examined for the development of $ICOS^+PD\text{-}1^+$ cTfh cells. Once detected on posttransplant day 7 (Figures 7A–D), immunosuppression was initiated with anti-CD28 dAb. Strikingly, delayed treatment with anti-CD28 CoB abrogated continued expansion and differentiation of donor-reactive cTfh cells and inhibited the development of DSA compared to untreated controls (Figures 7E, F). As with the initiation of treatment at the time of transplant (Figure 6), the rise and fall of the cTfh cell response was related to the formation of anti-donor antibodies. As such, immunosuppression initiated after the detection of alloreactive $ICOS^+PD\text{-}1^+$ cTfh cells in the blood successfully inhibited DSA formation.

4. Discussion

Circulating Tfh cells have been shown to correlate with autoimmune disease, vaccine responses and broadly neutralizing antibodies against HIV (26–29, 32). Their presence in the blood, relation to GC Tfh cells in SLOs, and ability to indicate GC reactivity has introduced the possibility of utilizing them as a biomarker for alloantibody responses in transplantation (11, 16). While Tfh cells have generated considerable interest in transplantation and have been implicated in anti-donor antibody responses (12–14, 33), little is known regarding the cTfh cell response to an allograft. Two observational studies have reported that $CXCR5^+$ $CD4^+$ T cells in the blood of kidney transplant recipients are present at higher frequencies in cases of chronic rejection and *de novo* DSA (17, 18), and a more recent study observed higher frequencies of cTfh cells in sensitized transplant recipients with greater expansion post-transplant in patients that developed *de novo* HLA antibodies (19). Conversely, reduced fractions of activated cTfh cells have been reported in operationally tolerant (34) and belatacept-treated (35) renal transplant recipients. While these studies suggest an association between cTfh cells and humoral alloimmune phenotype in human transplant recipients, experimental data examining the temporal relationship

between cTfh cells and alloantibody formation for their evaluation as a biomarker in transplantation are needed.

In this study, we provide experimental evidence that alloreactive, antigen-specific cTfh cells functionally capable of providing B cell help for antibody production are detectable in the blood and expand after transplant, correlate with ongoing GC alloreactivity in graft-dLNs and precede the manifestation of anti-donor antibodies. Intriguingly, we also observed temporal polarization of cTfh cells towards an activated $ICOS^+PD\text{-}1^+$ phenotype in an allo-dependent manner post-transplant that preceded DSA formation earlier than the quantitative rise in cTfh cells. Notably, the development of cTfh cells occurred in the context of modified and unmodified DSA formation (Figure 6), and the detection of $ICOS^+PD\text{-}1^+$ cTfh cells in the blood successfully prompted initiation of immunosuppression to prevent DSA (Figure 7).

Blood Tfh cells have been primarily characterized as antigen-experienced $CXCR5^+$ $CD4^+$ memory T cells that accumulate after repeated antigen exposures and have the ability to surveil SLOs with the purpose of accelerating memory antibody responses (36, 37). However, considerable phenotypic and functional heterogeneity has been observed within cTfh cells to suggest that the total pool of $CXCR5^+$ $CD4^+$ T cells is comprised of a variety of different subsets with varying degrees of differentiation that include both quiescent, memory-like subsets and more activated, effector-like subsets indicative of active Tfh cell differentiation in lymphoid organs (16, 30, 38). Thus, fluctuations in the composition of the cTfh cell pool may reflect periods of active humoral immune reactivity.

Several studies have demonstrated that the expression of ICOS and PD-1 on cTfh cells correlates with autoimmune disease activity and protective antibody responses following vaccination (27–29), and that the absence or low levels of ICOS or PD-1 on cTfh cells are indicative of a resting, inactive state. In clinical transplantation, allograft recipients with complex immune histories are likely to have heterogenous pools of polyreactive $CXCR5^+$ cTfh cell memory, where detecting acute shifts in the phenotypic composition of these blood Tfh cells may specifically indicate active humoral alloreactivity. While the observed changes in cTfh cells in this study are alloantigen-elicited, similar changes may occur to any antigen (i.e. infectious pathogens) that stimulates a GC-dependent antibody response. As such, continued investigation of activated cTfh cell subsets like the $ICOS^+PD\text{-}1^+$ subset recognized in this study may facilitate identification and tracking of allo-specific T cells responsible for alloantibody responses. Alternatively, examining the role of donor-reactive memory B cells in the blood may also aid in the identification of donor-specific cellular biomarkers of humoral sensitization (39, 40). In light of these considerations, our data on the manifestation of an alloreactive $ICOS^+PD\text{-}1^+$ cTfh cell population with increased expression of Ki-67, CD154 and other Tfh program-specific markers in response to an allogeneic skin graft is noteworthy and consistent with published observations, further supporting their potential as a biomarker for humoral alloimmunity.

Our findings are proof of concept that quantitative and qualitative changes in blood Tfh cells are a cellular indicator of alloantibody formation and could guide clinical management strategies to mitigate the negative impact of DSA following transplantation. While the period

between the detection of phenotypic changes in cTfh cells and the generation of DSA in our experimental mouse model of unmodified antibody formation is seven days and may afford enough of a clinical window to prevent alloantibodies in certain scenarios, the window of opportunity for intervention is very likely to be months or years in clinical transplantation under standard immunosuppression (3, 41).

Antibody-mediated injury and the emergence of *de novo* DSA in the clinic most often occur several years after transplant and have been associated with prior episodes of cellular rejection and subclinical histopathologic changes months to years before the serologic detection of DSA (5, 42). Thus in the presence of immunosuppression, a cTfh cell signature in the blood may be present and detectable during these protracted clinical periods of occult germinal center alloreactivity. In support of this hypothesis, the development of breakthrough DSA under modified conditions with tacrolimus or CTLA-4-Ig in this study was in fact preceded by cTfh cell changes in the blood more than 7 days prior to the detection of DSA (Figure 6). This observation supports the notion that changes in cTfh cells during episodes of allograft dysfunction or periodically over the course of a transplant could be used as an indicator of developing humoral alloimmunity before the serologic detection of alloantibodies. In fact, a recent study examining the relationship between memory B cells and antibody-mediated rejection identified donor-reactive memory B cells in the blood of kidney transplant recipients without DSA at the time of transplant 18 months prior to the diagnosis of subclinical ABMR and detection of serologic DSA (40). It is probable that the rate of Tfh cell differentiation, GC reactivity and the development of de novo DSA is a net result of the balance between the nature of alloantigen along with the immune environment, and the quantity and quality of immunosuppression.

Given the smoldering nature and lack of effective clinical therapies to combat alloantibody formation and DSA-mediated injury (3, 6, 42), the ability of delayed immunosuppression initiated upon identification of alloreactive $ICOS^{+}PD\text{-}1^{+}$ cTfh cells before the development of DSA to inhibit the humoral response is of clinical interest. Young et al. have previously shown that delayed treatment with a higher dose and greater frequency of CTLA-4-Ig administration also reversed ongoing alloantibody responses in a mouse heterotopic heart transplant model (43), but delayed treatment was arbitrarily initiated and not prompted by the identification of a potential biomarker as in this study. These findings are crucial to considering the clinical applicability and potential translation of cTfh cells as a biomarker for humoral alloimmune monitoring in transplant recipients, and also supports the use of CoB as rescue therapy to prevent DSA.

The use of a non-vascularized skin graft model in these studies could have translational implications. Differences in the mode of transplant revascularization, lymphatic drainage, tissue-specific antigens, graft immunogenicity, and graft size are all variables known to influence the nature of an alloimmune response (44). As such, the presence of professional antigen presenting Langerhans cells in the skin with the ability to accelerate T cell stimulation in SLOs (45) and the increased ischemia that results in greater inflammation and necrosis in non-vascularized grafts, along with alterations in leukocyte trafficking in the absence of vascular endothelium, could significantly impact the magnitude and quality of Tfh cell-mediated alloantibody formation and cTfh cell kinetics. While the consistency of

our results with published observations on cTfh cells in a variety of experimental models and humans with different methods of antigen exposure and disease processes support the relevance of our findings (15, 16, 27), the skin allograft model employed in this study should be considered in the application of our observations to vascularized grafts.

In summary, this study provides evidence that quantitative and phenotypic changes in alloreactive, donor-specific cTfh cells in the blood of transplanted mice indicate GC alloreactivity and precede *de novo* DSA formation. Our data highlight the potential for cTfh cells to be utilized as a predictive biomarker for humoral alloreactivity and the generation of DSA in clinical transplantation that could trigger the initiation of therapy to prevent alloantibody-mediated allograft injury. These findings support additional investigation of cTfh cells in vascularized transplant models and humans to enhance their applicability as a clinically relevant cellular biomarker for the diagnosis or prediction of HLA antibody-mediated processes in transplantation.

Acknowledgments

The authors would like to thank Drs. S. G. Nadler and S. J. Suchard at Bristol-Myers Squibb for providing the anti-CD28 dAb. Grants T32 AI070081 and F31 AI145178 (G.M.L), R01s AI073707 and AI104699 (M.L.F.), K08 AI132747 (I.R.B.), and an Emory University Research Committee Award (I.R.B.) supported this work.

Abbreviations:

CoB	costimulation blockade
cTfh	circulating T follicular helper
dAb	domain antibody
dLN	draining lymph node
DSA	donor-specific antibody
GC	germinal center
mOVA	membrane-bound ovalbumin
OVA	ovalbumin
PBMC	peripheral blood mononuclear cells
SLO	secondary lymphoid organ
TCR	T cell receptor
Tfh	T follicular helper

References

1. Hart A, Smith JM, Skeans MA, Gustafson SK, Wilk AR, Robinson A, et al. OPTN/SRTR 2016 Annual Data Report: Kidney. Am J Transplant. 2018;18 Suppl 1:18–113. [PubMed: 29292608]
2. Nankivell BJ, Borrows RJ, Fung CL, O'Connell PJ, Allen RD, Chapman JR. The natural history of chronic allograft nephropathy. N Engl J Med. 2003;349(24):2326–33. [PubMed: 14668458]

3. Loupy A, Hill GS, Jordan SC. The impact of donor-specific anti-HLA antibodies on late kidney allograft failure. Nat Rev Nephrol. 2012;8(6):348–57. [PubMed: 22508180]
4. Lefaucheur C, Loupy A, Hill GS, Andrade J, Nochy D, Antoine C, et al. Preexisting donor-specific HLA antibodies predict outcome in kidney transplantation. J Am Soc Nephrol. 2010;21(8):1398–406. [PubMed: 20634297]
5. Wiebe C, Gibson IW, Blydt-Hansen TD, Karpinski M, Ho J, Storsley LJ, et al. Evolution and clinical pathologic correlations of de novo donor-specific HLA antibody post kidney transplant. Am J Transplant. 2012;12(5):1157–67. [PubMed: 22429309]
6. Djamali A, Kaufman DB, Ellis TM, Zhong W, Matas A, Samaniego M. Diagnosis and management of antibody-mediated rejection: current status and novel approaches. Am J Transplant. 2014;14(2):255–71. [PubMed: 24401076]
7. Bray RA, Gebel HM. Strategies for human leukocyte antigen antibody detection. Curr Opin Organ Transplant. 2009;14(4):392–7. [PubMed: 19610172]
8. Bray RA, Gebel HM. Monitoring after renal transplantation: recommendations and caveats. Nat Clin Pract Nephrol. 2008;4(12):658–9. [PubMed: 18852733]
9. Viglietti D, Loupy A, Vernerey D, Bentlejewski C, Gosset C, Aubert O, et al. Value of Donor-Specific Anti-HLA Antibody Monitoring and Characterization for Risk Stratification of Kidney Allograft Loss. J Am Soc Nephrol. 2017;28(2):702–15. [PubMed: 27493255]
10. Crotty S. Follicular helper CD4 T cells (TFH). Annu Rev Immunol. 2011;29:621–63. [PubMed: 21314428]
11. Crotty S. T follicular helper cell differentiation, function, and roles in disease. Immunity. 2014;41(4):529–42. [PubMed: 25367570]
12. Conlon TM, Saeb-Parsy K, Cole JL, Motallebzadeh R, Qureshi MS, Rehakova S, et al. Germinal Center Alloantibody Responses Are Mediated Exclusively by Indirect-Pathway CD4 T Follicular Helper Cells. Journal of Immunology. 2012;188(6):2643–52.
13. Kim EJ, Kwun J, Gibby AC, Hong JJ, Farris AB 3rd, Iwakoshi NN, et al. Costimulation blockade alters germinal center responses and prevents antibody-mediated rejection. Am J Transplant. 2014;14(1):59–69. [PubMed: 24354871]
14. Badell IR, La Muraglia GM 2nd, Liu D, Wagener ME, Ding G, Ford ML. Selective CD28 Blockade Results in Superior Inhibition of Donor-Specific T Follicular Helper Cell and Antibody Responses Relative to CTLA4-Ig. Am J Transplant. 2018;18(1):89–101. [PubMed: 28637095]
15. Tangye SG, Ma CS, Brink R, Deenick EK. The good, the bad and the ugly – TFH cells in human health and disease. Nat Rev Immunol. 2013;13(6):412–26. [PubMed: 23681096]
16. Ueno H. Human Circulating T Follicular Helper Cell Subsets in Health and Disease. J Clin Immunol. 2016;36 Suppl 1:34–9. [PubMed: 26984851]
17. de Graav GN, Dieterich M, Hesselink DA, Boer K, Clahsen-van Groningen MC, Kraaijeveld R, et al. Follicular T helper cells and humoral reactivity in kidney transplant patients. Clin Exp Immunol. 2015;180(2):329–40. [PubMed: 25557528]
18. Shi J, Luo F, Shi Q, Xu X, He X, Xia Y. Increased circulating follicular helper T cells with decreased programmed death-1 in chronic renal allograft rejection. BMC Nephrol. 2015;16:182. [PubMed: 26525294]
19. Cano-Romero FL, Laguna Goya R, Utrero-Rico A, Gomez-Massa E, Arroyo-Sanchez D, Suarez-Fernandez P, et al. Longitudinal profile of circulating T follicular helper lymphocytes parallels anti-HLA sensitization in renal transplant recipients. Am J Transplant. 2019;19(1):89–97. [PubMed: 29947147]
20. Hogquist KA, Jameson SC, Heath WR, Howard JL, Bevan MJ, Carbone FR. T cell receptor antagonist peptides induce positive selection. Cell. 1994;76(1):17–27. [PubMed: 8287475]
21. Barnden MJ, Allison J, Heath WR, Carbone FR. Defective TCR expression in transgenic mice constructed using cDNA-based alpha- and beta-chain genes under the control of heterologous regulatory elements. Immunol Cell Biol. 1998;76(1):34–40. [PubMed: 9553774]
22. Ehst BD, Ingulli E, Jenkins MK. Development of a novel transgenic mouse for the study of interactions between CD4 and CD8 T cells during graft rejection. Am J Transplant. 2003;3(11):1355–62. [PubMed: 14525595]

23. Trambley J, Bingaman AW, Lin A, Elwood ET, Waitze SY, Ha J, et al. Asialo GM1(+) CD8(+) T cells play a critical role in costimulation blockade-resistant allograft rejection. J Clin Invest. 1999;104(12):1715–22. [PubMed: 10606625]
24. Sage PT, Sharpe AH. In vitro assay to sensitively measure T(FR) suppressive capacity and T(FH) stimulation of B cell responses. Methods Mol Biol. 2015;1291:151–60. [PubMed: 25836309]
25. Choi YS, Gullicksrud JA, Xing S, Zeng Z, Shan Q, Li F, et al. LEF-1 and TCF-1 orchestrate T(FH) differentiation by regulating differentiation circuits upstream of the transcriptional repressor Bcl6. Nat Immunol. 2015;16(9):980–90. [PubMed: 26214741]
26. Morita R, Schmitt N, Bentebibel S-E, Ranganathan R, Bourdery L, Zurawski G, et al. Human Blood CXCR5+CD4+ T Cells Are Counterparts of T Follicular Cells and Contain Specific Subsets that Differentially Support Antibody Secretion. Immunity. 2011;34(1):108–21. [PubMed: 21215658]
27. He J, Tsai LM, Leong YA, Hu X, Ma CS, Chevalier N, et al. Circulating precursor CCR7(lo)PD-1(hi) CXCR5(+) CD4(+) T cells indicate Tfh cell activity and promote antibody responses upon antigen reexposure. Immunity. 2013;39(4):770–81. [PubMed: 24138884]
28. Locci M, Havenar-Daughton C, Landais E, Wu J, Kroenke MA, Arlehamn CL, et al. Human circulating PD-1+CXCR3-CXCR5+ memory Tfh cells are highly functional and correlate with broadly neutralizing HIV antibody responses. Immunity. 2013;39(4):758–69. [PubMed: 24035365]
29. Bentebibel SE, Lopez S, Obermoser G, Schmitt N, Mueller C, Harrod C, et al. Induction of ICOS +CXCR3+CXCR5+ TH cells correlates with antibody responses to influenza vaccination. Sci Transl Med. 2013;5(176):176ra32.
30. Schmitt N, Ueno H. Blood Tfh cells come with colors. Immunity. 2013;39(4):629–30. [PubMed: 24138878]
31. Ford ML, Koehn BH, Wagener ME, Jiang W, Gangappa S, Pearson TC, et al. Antigen-specific precursor frequency impacts T cell proliferation, differentiation, and requirement for costimulation. J Exp Med. 2007;204(2):299–309. [PubMed: 17261633]
32. Singh D, Henkel M, Sendon B, Feng J, Fabio A, Metes D, et al. Analysis of CXCR5(+)Th17 cells in relation to disease activity and TNF inhibitor therapy in Rheumatoid Arthritis. Sci Rep. 2016;6:39474. [PubMed: 28004828]
33. Badell IR, Ford ML. T follicular helper cells in the generation of alloantibody and graft rejection. Curr Opin Organ Transplant. 2016;21(1):1–6. [PubMed: 26727455]
34. Chenouard A, Chesneau M, Bui Nguyen L, Le Bot S, Cadoux M, Dugast E, et al. Renal Operational Tolerance Is Associated With a Defect of Blood Tfh Cells That Exhibit Impaired B Cell Help. Am J Transplant. 2017;17(6):1490–501. [PubMed: 27888555]
35. Leibler C, Thiolat A, Henique C, Samson C, Pilon C, Tamagne M, et al. Control of Humoral Response in Renal Transplantation by Belatacept Depends on a Direct Effect on B Cells and Impaired T Follicular Helper-B Cell Crosstalk. J Am Soc Nephrol. 2018;29(3):1049–62. [PubMed: 29321143]
36. Hale JS, Youngblood B, Latner DR, Mohammed AU, Ye L, Akondy RS, et al. Distinct memory CD4+ T cells with commitment to T follicular helper- and T helper 1-cell lineages are generated after acute viral infection. Immunity. 2013;38(4):805–17. [PubMed: 23583644]
37. Sage PT, Alvarez D, Godec J, von Andrian UH, Sharpe AH. Circulating T follicular regulatory and helper cells have memory-like properties. J Clin Invest. 2014;124(12):5191–204. [PubMed: 25347469]
38. Hale JS, Ahmed R. Memory T follicular helper CD4 T cells. Front Immunol. 2015;6:16. [PubMed: 25699040]
39. Lucia M, Luque S, Crespo E, Melilli E, Cruzado JM, Martorell J, et al. Preformed circulating HLA-specific memory B cells predict high risk of humoral rejection in kidney transplantation. Kidney Int. 2015;88(4):874–87. [PubMed: 26176829]
40. Luque S, Lucia M, Melilli E, Lefaucheur C, Crespo M, Loupy A, et al. Value of monitoring circulating donor-reactive memory B cells to characterize antibody-mediated rejection after kidney transplantation. Am J Transplant. 2019;19(2):368–80. [PubMed: 30085394]

41. Wiebe C, Gibson IW, Blydt-Hansen TD, Pochinco D, Birk PE, Ho J, et al. Rates and determinants of progression to graft failure in kidney allograft recipients with de novo donor-specific antibody. Am J Transplant. 2015;15(11):2921–30. [PubMed: 26096305]

42. Nickerson PW, Rush DN. Begin at the Beginning to Prevent the End. J Am Soc Nephrol. 2015;26(7):1483–5. [PubMed: 25556171]

43. Young JS, Chen J, Miller ML, Vu V, Tian C, Moon JJ, et al. Delayed Cytotoxic T Lymphocyte-Associated Protein 4-Immunoglobulin Treatment Reverses Ongoing Alloantibody Responses and Rescues Allografts From Acute Rejection. Am J Transplant. 2016;16(8):2312–23. [PubMed: 26928966]

44. Jones ND, Turvey SE, Van Maurik A, Hara M, Kingsley CI, Smith CH, et al. Differential susceptibility of heart, skin, and islet allografts to T cell-mediated rejection. J Immunol. 2001;166(4):2824–30. [PubMed: 11160350]

45. Larsen CP, Steinman RM, Witmer-Pack M, Hankins DF, Morris PJ, Austyn JM. Migration and maturation of Langerhans cells in skin transplants and explants. J Exp Med. 1990;172(5):1483–93. [PubMed: 2230654]

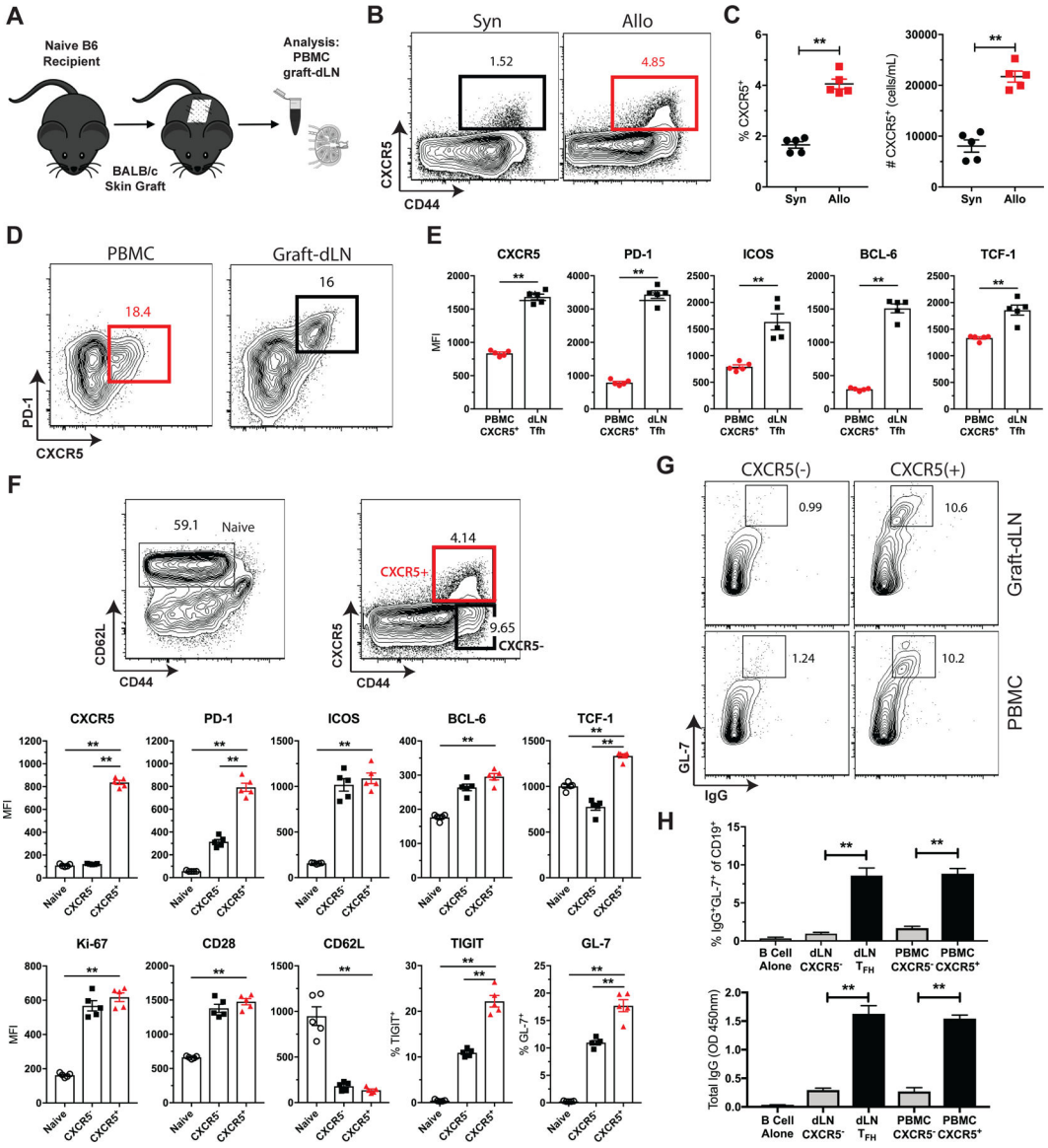

Figure 1. Circulating CXCR5$^+$ CD4$^+$ T cells expand following transplantation and display phenotypic and functional characteristics of cTfh cells.

(A) Naïve B6 mice were transplanted with skin from either B6 (Syn) or BALB/c (Allo) donors and sacrificed 10 days post-transplantation for PBMC and graft-dLN analysis. (B) Flow cytometric plots (gated on CD4$^+$Foxp3$^-$ T cells) displaying the frequencies of CXCR5$^+$ T cells. (C) Summary data of the frequencies and numbers of cTfh cells (n=5 per group). (D) Representative flow plots (gated on CD4$^+$Foxp3$^-$ T cells) of blood-derived CXCR5$^+$ (PBMC) and graft-dLN Tfh cells as defined by CXCR5 and PD-1. (E) Summary data of phenotypic marker expression by CXCR5$^+$ PBMCs and graft-dLN Tfh cells (n=5 per group). (F) Flow plots (gated on CD4$^+$Foxp3$^-$ T cells) depict gating strategy for naïve (CD44^{lo}CD62L$^+$), antigen-experienced (CD44^{hi}CXCR5$^-$) and CXCR5$^+$ T cell populations with summary data of phenotypic marker expression by each subset, respectively (n=5 per group). (G) Representative flow plots (gated on CD19$^+$IA-IE$^+$ B Cells) displaying the frequencies of GC-like B cells following 6-day *in vitro* T:B cell co-culture from BALB/c

transplanted mice. (H) Summary data of the frequencies of $IgG^+GL\text{-}7^+$ B cells and total IgG after T:B cell co-culture (n=3 with cells pooled from 5–10 mice). Summary data represent mean (SE) and are representative of 2–4 independent experiments with a total of 10–20 mice per group. *p < 0.05, **p < 0.01, ***p< 0.001.

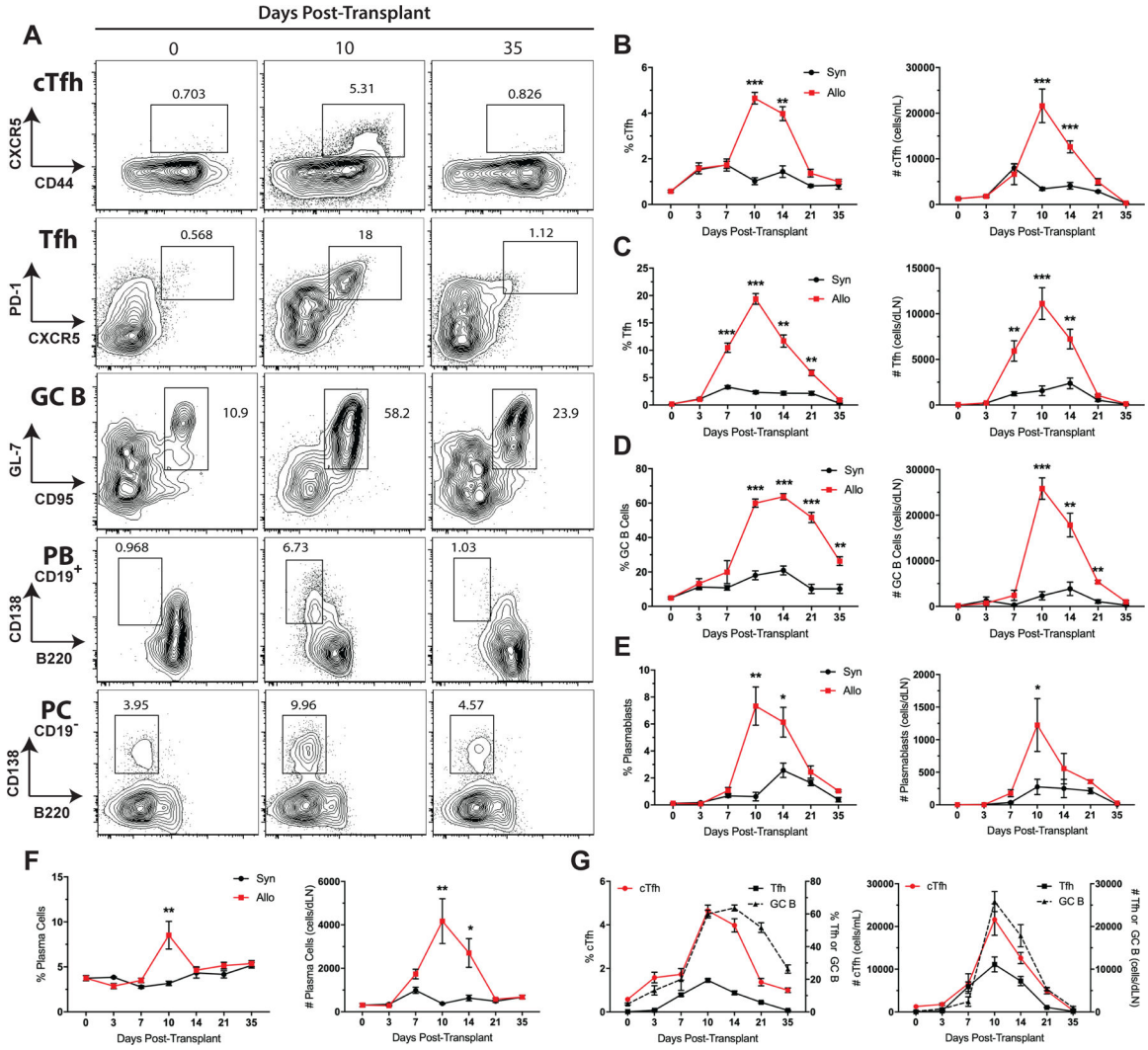

Figure 2. Circulating Tfh cell kinetics parallel graft-dLN GC reactivity following transplantation.

Naïve B6 mice were transplanted with skin from either B6 (Syn) or BALB/c (Allo) donors and serially sacrificed post-transplantation for PBMC and graft-dLN analysis. (A) Representative flow plots displaying the frequencies of blood cTfh (gated on $CD4^{+}Foxp3^{-}$ T cells), graft-dLN Tfh (gated on $CD4^{+}Foxp3^{-}CD44^{hi}$ T cells), GC B (gated on $CD19^{+}IgD^{-}B220^{+}CD138^{-}$ B cells), plasmablast (gated on $CD19^{+}IgD^{-}$ cells), and plasma (gated on $CD19^{-}IgD^{-}$ cells) cells over time. Summary data of (B) cTfh cell, (C) graft-dLN Tfh cell, (D) GC B cell, (E) plasmablast, and (F) plasma cell frequencies and numbers over time (n=5 per group). (G) Summary data of cTfh cell frequencies and numbers relative to graft-dLN Tfh and GC B cell frequencies and numbers, respectively (n=5 per group). Summary data represent mean (SE) and are representative of three independent experiments with a total of 15 mice per group. *$p < 0.05$, **$p < 0.01$, ***$p < 0.001$.

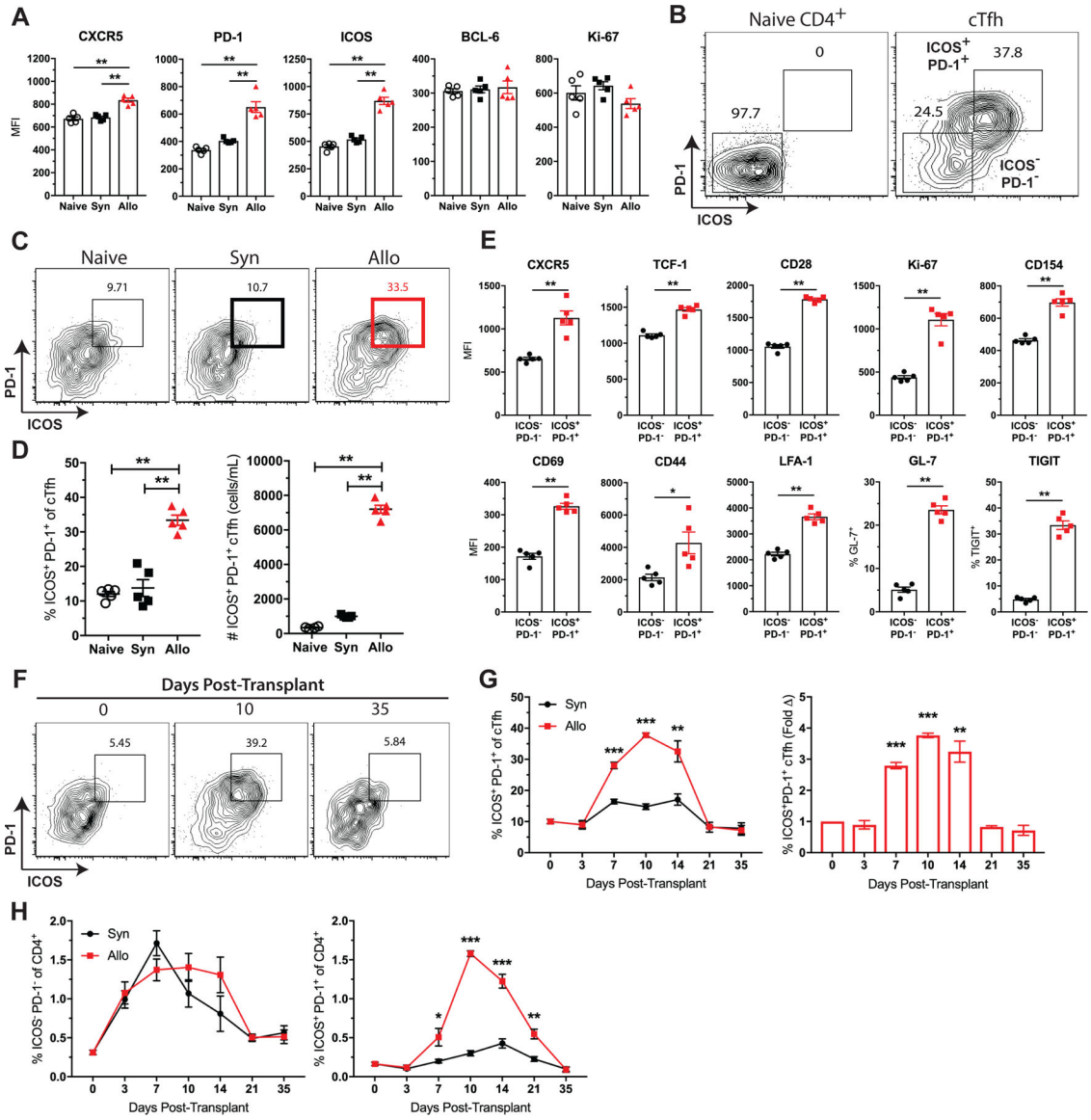

Figure 3. Donor-reactive cTfh cells exhibit an activated ICOS$^+$PD-1$^+$ phenotype after transplantation.

Naïve B6 mice were transplanted with skin from either B6 (Syn) or BALB/c (Allo) donors and sacrificed for PBMC analysis. (A) Summary data of phenotypic marker expression on cTfh cells from naïve, syngeneic and allogeneic skin-grafted mice ten days after transplant (n=5 per group). (B) Representative flow plots depicting ICOS and PD-1 expression on naïve (CD44^{lo}CD62L$^+$) CD4$^+$ T cells and CXCR5$^+$ cTfh cells. (C) Representative flow plots (gated on CD4$^+$Foxp3$^-$CXCR5$^+$ T cells) displaying the frequencies of ICOS$^+$PD-1$^+$ cTfh cells. (D) Summary data of the frequencies and numbers of ICOS$^+$PD-1$^+$ cTfh cells (n=5 per group). (E) Summary data of phenotypic marker expression on ICOS$^-$PD-1$^-$ and ICOS$^+$PD-1$^+$ cTfh cells (n=5 per group). (F) Representative flow plots (gated on CD4$^+$CXCR5$^+$ T cells) displaying the frequencies of ICOS$^+$PD-1$^+$ cTfh cells over time. (G) Summary data of ICOS$^+$PD-1$^+$ cTfh cell frequencies and fold change over time (n=5 per group). (H) Summary data of ICOS$^-$PD-1$^-$ and ICOS$^+$PD-1$^+$ cTfh cell frequencies of CD4$^+$ T cells over

time. Summary data represent mean (SE) and are representative of 3–4 independent experiments with a total of 15–20 mice per group. *p < 0.05, **p < 0.01, ***p< 0.001.

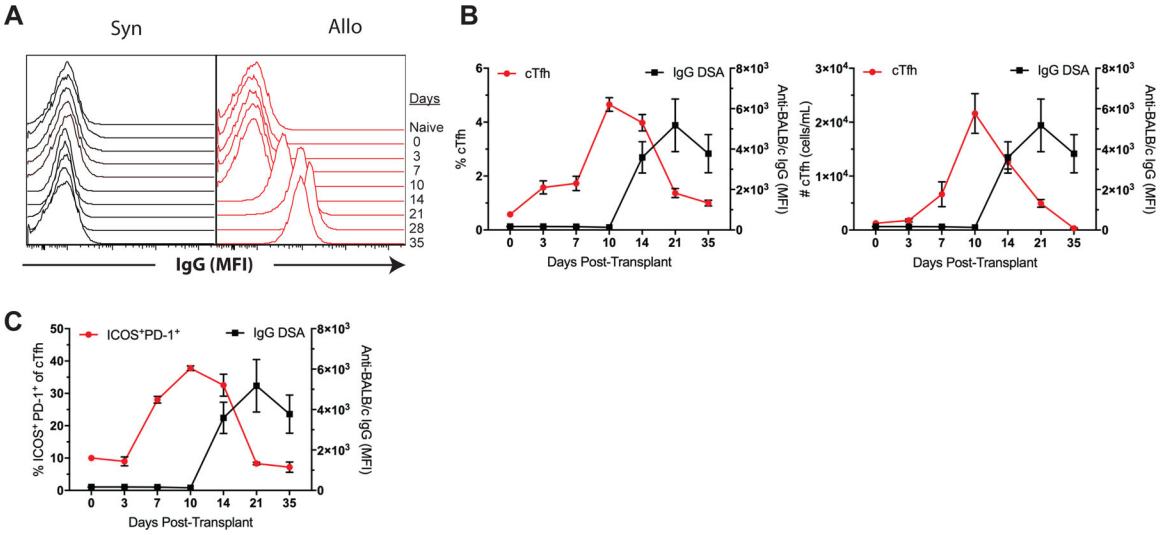

Figure 4. Circulating Tfh cells precede DSA formation following transplantation.

Naïve B6 mice were transplanted with skin from either B6 (Syn) or BALB/c (Allo) donors and serially bled for serum collection and flow crossmatch analysis. (A) Representative histograms of anti-donor IgG in syngeneic and allogeneic skin-grafted mice over time. (B) Summary data of cTfh cell frequencies and numbers relative to anti-donor IgG over time (n=5 per group). (C) Summary data of $ICOS^{+}PD\text{-}1^{+}$ cTfh cell frequencies relative to DSA formation over time (n=5 per group). Summary data represent mean (SE) and are representative of three independent experiments with a total of 15 mice per group. *$p < 0.05$, **$p < 0.01$, ***$p< 0.001$.

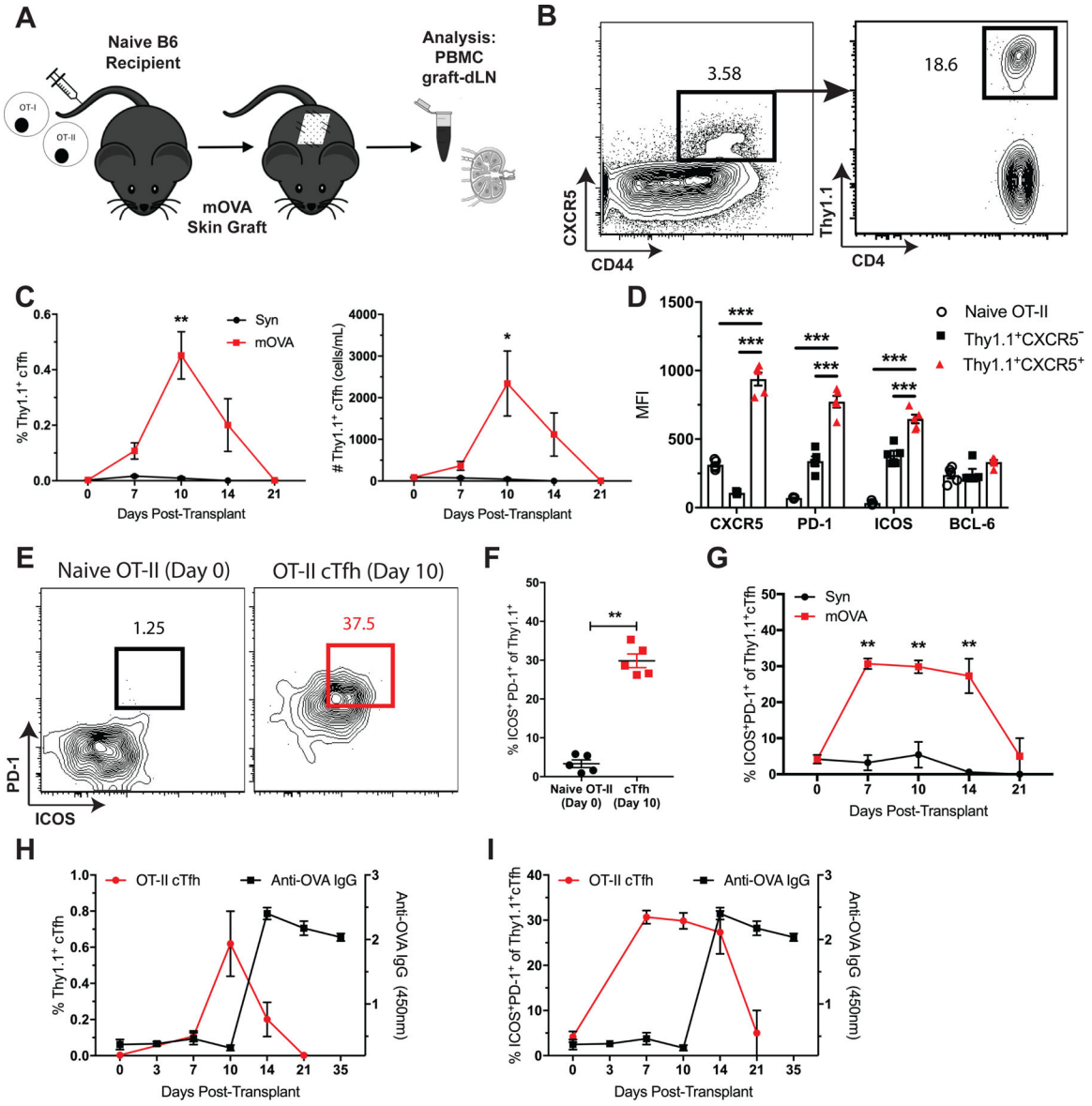

Figure 5. Antigen-specific TCR transgenic cTfh cells display similar phenotypic characteristics and kinetics to endogenous alloreactive cTfh cells following transplantation.

(A) Naïve B6 mice were adoptively transferred 10^6 of each Thy1.1$^+$ CD4$^+$ OT-II and CD8$^+$ OT-I T cells, transplanted skin from B6 (Syn) or mOVA donors and sacrificed at indicated time points post-transplantation for PBMC, graft-dLN and serum analyses. (B) Flow plots (gated on CD4$^+$Foxp3$^-$ T cells) depict gating strategy for CXCR5$^+$Thy1.1$^+$ OVA-specific cTfh cells. (C) Summary data of Thy1.1$^+$ cTfh cell frequencies and numbers following B6 (Syn) or mOVA skin transplantation over time (n=5 per group). (D) Summary data of phenotypic marker expression in naïve (CD44^{lo}CD62L$^+$) OT-II cells, and Thy1.1$^+$ CXCR5$^-$ or CXCR5$^+$ OT-II cells from the peripheral blood 10 days post-transplantation (n=5 per group). (E) Flow plots depicting ICOS and PD-1 expression on naive OT-II cells on day 0 and Thy1.1$^+$CXCR5$^+$ cTfh cells 10 days post-transplantation. (F) Summary data of the frequencies of ICOS$^+$PD-1$^+$ of naïve OT-II cells on day 0 and Thy1.1$^+$ cTfh cells 10 days

after transplant (n=5 per group). (G) Summary data of $ICOS^+PD\text{-}1^+$ $Thy1.1^+$ cTfh cell frequencies over time (n=5 per group). Summary data of (H) $Thy1.1^+$ cTfh cell and (I) $ICOS^+PD\text{-}1^+$ $Thy1.1^+$ cTfh cell frequencies relative to anti-OVA IgG formation over time (n=5 per group). Summary data represent mean (SE) and are representative of three independent experiments with a total of 10–15 mice per group. *$p < 0.05$, **$p < 0.01$, ***$p< 0.001$.

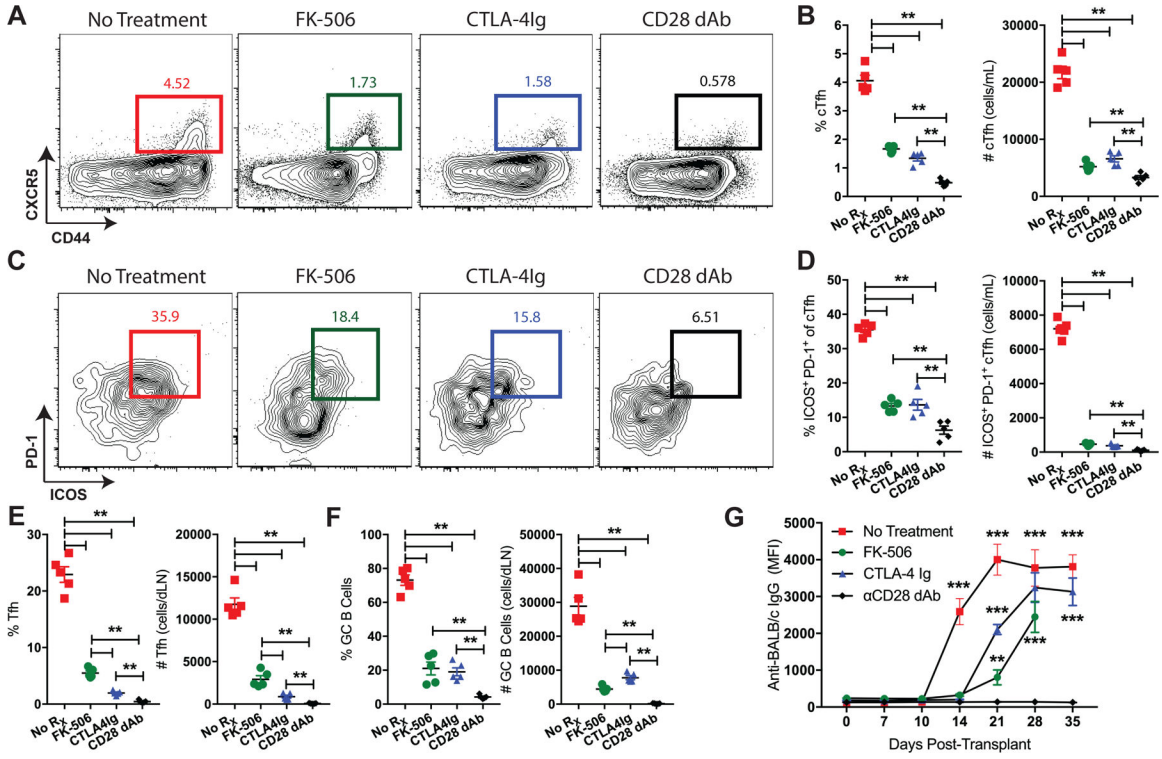

Figure 6. Circulating Tfh cells predict breakthrough alloantibodies despite immunosuppression.

Naïve B6 mice were transplanted with BALB/c skin grafts and treated with tacrolimus (FK-506), CTLA-4-Ig, anti-CD28 dAb, or left untreated. BALB/c-grafted mice were sacrificed 10 days post-transplant for PBMC and graft-dLN analysis and serially bled for DSA assessment. (A) Representative flow cytometric plots (gated on $CD4^{+}Foxp3^{-}$ T cells) displaying the frequencies of $CXCR5^{+}$ cTfh cells. (B) Summary data of the frequencies and numbers of cTfh cells (n=5 per group). (C) Representative flow plots (gated on $CD4^{+}Foxp3^{-}CXCR5^{+}$ T cells) displaying the frequencies of $ICOS^{+}PD\text{-}1^{+}$ cTfh cells. (D) Summary data of the frequencies and numbers of $ICOS^{+}PD\text{-}1^{+}$ cTfh cells (n=5 per group). Summary data of the frequencies and numbers of graft-dLN (E) Tfh and (F) GC B cells (n=5 per group). (G) Summary data of anti-donor IgG formation in treated or untreated BALB/c-grafted mice over time (n=5 per group). Summary data represent mean (SE) and are representative of three independent experiments with a total of 15 mice per group. *p < 0.05, **p < 0.01, ***p< 0.001.

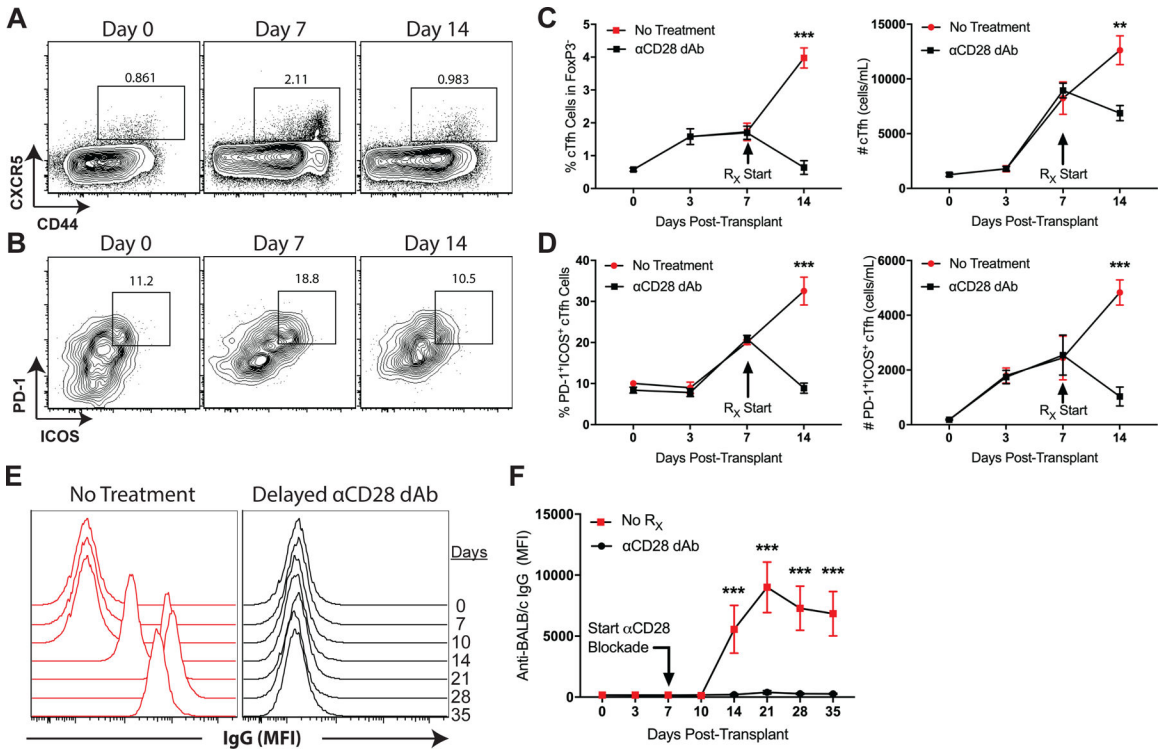

Figure 7. Delayed anti-CD28 CoB initiated after detection of ICOS$^+$PD-1$^+$ cTfh cells prevents DSA formation.

Naïve B6 mice were transplanted BALB/c skin grafts and their blood serially monitored for the development of ICOS$^+$PD-1$^+$ cTfh cells. Once detected on post-transplant day 7, immunosuppression with anti-CD28 dAb was initiated. Representative flow plots (gated on CD4$^+$Foxp3$^-$ T cells) displaying the frequencies of (A) cTfh and (B) ICOS$^+$PD-1$^+$ cTfh cells over time. Summary data of the frequencies and numbers of (C) cTfh and (D) ICOS$^+$PD-1$^+$ cTfh cells (n=5 per group). (E) Representative histograms of anti-donor IgG in untreated and delayed anti-CD28 dAb treated mice over time. (F) Summary data of anti-donor IgG over time (n=5 per group). Summary data represent mean (SE) and are representative of two independent experiments with a total of 10 mice per group. *$p < 0.05$, **$p < 0.01$, ***$p< 0.001$.